X-ray double and triple crystal diffractometry of mosaic structure in heteroepitaxial layers

V. Holý and J. Kuběna
Department of Solid State Physics, Faculty of Science, the Masaryk University, Kotlářská 2, 611 37 Brno, Czech Republic

E. Abramof,[a] K. Lischka, and A. Pesek
Institute of Optoelectronics, the Kepler University, Altenbergerstrasse 69, 4040 Linz, Austria

E. Koppensteiner
Institute of Semiconductor Physics, the Kepler University, Altenbergerstrasse 69, 4040 Linz, Austria

(Received 4 November 1992; accepted for publication 8 April 1993)

X-ray diffraction in thin layers containing small randomly placed defects is described by means of the kinematical diffraction theory and optical coherence formalism. The method enables us to calculate both the diffracted intensity and its angular distribution, so that it can be used for simulating double crystal and triple crystal x-ray diffractometry experiments. The theory has been applied to experimental data obtained from diffractometry measurements of an epitaxial ZnTe layer with mosaic structure after several steps of chemical thinning. A good agreement of the theory with experiments has been achieved.

I. INTRODUCTION

X-ray diffractometry is a powerful tool for characterizing the structure of thin monocrystalline layers. It is frequently used for determining the lattice parameters of the layer and the layer thickness. The crystalline quality of the layer has been characterized mainly by measuring the width of the rocking curve (FWHM) by means of x-ray double crystal diffractometry (DC).[1–3] From the FWHM the dislocation density can be determined.[4] This approach, however, has been developed for polycrystalline samples and in the case of single crystals it can only be used for a rough estimate.

Triple crystal diffractometry (TC) is frequently used for investigating the x-ray diffuse scattering. It has been demonstrated[5–8] that contour maps of diffuse scattering measured near the reciprocal lattice point (RELP) are related with the defect structure of the sample.

Structural defects in heteroepitaxial layers are caused mainly by threading dislocations and their climb.[9] They are generated by a coalescence process of seed islands occurring during a three-dimensional layer growth at the substrate surface. The crystallographic structure of relaxed heteroepitaxial layers can be modeled by the conception of mosaic structure. The mosaic block size corresponds with the mean distance between threading dislocations.

The aim of this paper is to present a theoretical approach enabling us to calculate both the DC reflection curves and the TC contour maps of thin layers with randomly distributed small defects. We demonstrate that analyzing the entire form of a DC reflection curve we can get more information about the defects than using only FWHM. The general theory is used for calculating the DC reflection curves and TC contour maps of thin epitaxial layers with mosaic structure and the results are compared with DC and TC measurements of a ZnTe epitaxial layer grown on a GaAs substrate.

II. X-RAY DIFFRACTION IN DISTORTED CRYSTALS

We restrict ourselves to the kinematical diffraction theory. This simplification can be performed if the total crystal thickness T is much smaller than the x-ray extinction length. In the case of diffraction on a thin distorted layer lying on a thick (or semi-infinite) substrate this approach is applicable if we do not consider the diffraction in the substrate, i.e., the substrate must not diffract if the layer is in the diffraction position. The kinematical diffraction in a thin layer is equivalent with the first Born approximation in the scattering theory. The diffracted wave in an observation point $\mathbf{R}$ can be expressed as[10]

$$D(\mathbf{R}) = C r_{\mathrm{el}} \int_V d\mathbf{r}\, \rho(\mathbf{r})\, D_{\mathrm{inc}}(\mathbf{r})\, G_{\mathrm{free}}(\mathbf{R}-\mathbf{r}), \qquad (1)$$

where $\rho(\mathbf{r})$ is the electron density in point $\mathbf{r}$ inside the crystal, r_{el} is the classical electron radius ($r_{\mathrm{el}}=e^2/mc^2$ in CGSE units), C is the polarization factor of the incident wave D_{inc}, and G_{free} is the Green function of a free particle[10]

$$G_{\mathrm{free}} = \frac{\exp(-2\pi i k|\mathbf{R}-\mathbf{r}|)}{|\mathbf{R}-\mathbf{r}|}.$$

In the following we assume a plane incident wave

$$D_{\mathrm{inc}}(\mathbf{r}) = D_{\mathrm{inc}} \exp(-2\pi i \mathbf{k}_0 \cdot \mathbf{r}),$$

k is the length of the wave vector in the crystal ($k=Kn$, n is the refractive index of x-rays, $K=1/\lambda$ is the wave vector length in vacuum). We assumed $k_0=k$, i.e., in (1) x-ray

[a]Permanent address: Instituto de Pesquisas Espaciais, CP 515, 12201-S.J.Campos, SP, Brazil.

 0021-8979/93/74(3)/1736/8/$6.00

refraction is taken into account for the incident wave. The wave vector of the primary (vacuum) wave is $\mathbf{K}_0=\mathbf{k}_0-\boldsymbol{\delta}$, where $|\mathbf{K}_0|=K$ and vector $\boldsymbol{\delta}$ is perpendicular to the crystal surface. If we denote $\mathbf{K}_0^B$ the primary wave vector in the Bragg position, then

$$\mathbf{K}_0=\mathbf{K}_0^B+\boldsymbol{\kappa}_0$$

holds, where $\boldsymbol{\kappa}_0$ is the deviation of the primary wave vector from its Bragg position. Its length depends on the angular deviation ω of the crystal from the Bragg position and for small deviations it is perpendicular to $\mathbf{K}_0^B$.

Integration in (1) is performed over the whole irradiated volume V of the layer.

In the case of an ideal crystal $\rho(\mathbf{r})$ can be written as a Fourier series

$$\rho(\mathbf{r})=\rho_{\mathrm{id}}(\mathbf{r})=\sum_g \rho_g \exp(-2\pi i\mathbf{g}\cdot\mathbf{r}) \tag{2}$$

over the translation vectors $\mathbf{g}$ of the reciprocal ideal lattice.

Considering real crystals, we restrict ourselves to the Takagi approximation.[11] Its essence consists of the assumption that the crystal deformation only influences the phase terms $\exp(-2\pi i\mathbf{g}\cdot\mathbf{r})$, and the coefficients ρ_g are unchanged. This is valid if the components of the deformation tensor are much smaller than unity. Then

$$\rho(\mathbf{r})=\sum_g \rho_g \exp[-2\pi i\mathbf{g}\cdot(\mathbf{r}-\mathbf{u}(\mathbf{r}))] \tag{3}$$

holds, where $\mathbf{u}(\mathbf{r})$ is the displacement of the atom in point $\mathbf{r}$.

Putting (3) or (2) into (1) we get an explicit formula for $D(\mathbf{R})$. As usual, we could assume the validity of the Fraunhofer approximation[12] (for $|\mathbf{r}|\ll|\mathbf{R}|$) and we linearize the phase term in the Green function G_{free}. Within this approach, the entire scattering crystal is treated as a point source, therefore, even if the crystal is irradiated by a plane monochromatic wave, the diffracted wave is spherical. Obviously, this approach cannot be used if the diffracting crystal has a form of a thin large plate.

Ignoring the Fraunhofer approximation Eq. (1) can be simplified within the Takagi approximation. Then the function $\exp[2\pi i\mathbf{g}\cdot\mathbf{u}(\mathbf{r})]$ changes very slowly compared with the phase terms $\exp(-2\pi i\mathbf{g}\cdot\mathbf{r})$ and $\exp(-2\pi ikr)$. The integral in (1) can be evaluated by means of the two-dimensional stationary phase method.[13] After some algebra we get

$$D(\mathbf{R})=D_{\mathrm{inc}}Cr_{\mathrm{el}}/K\sum_g \exp[i\Phi(\mathbf{R},\mathbf{k}_g)]\rho_g\int_{l_g(\mathbf{R})} d\mathbf{r}$$
$$\times\exp(\pi iK\beta_g z/\gamma_g)\exp[2\pi i\mathbf{g}\cdot\mathbf{u}(\mathbf{r})]. \tag{4}$$

The integrals on the right-hand side are performed over lines $l_g(\mathbf{R})$ going through the observation point $\mathbf{R}$ in the direction of the diffracted wave with the wave vector

$$\mathbf{k}_g=\mathbf{k}_0+\mathbf{g}.$$

The positive z axis is parallel to the inward surface normal of the crystal, the x axis lies at the crystal surface in the plane of incidence. The phase term $\Phi(\mathbf{R},\mathbf{k}_g)$ only depends on the observation point and on the deviation ω. Its form is rather complicated and it is not substantial in the following considerations. Φ can be simplified if the observation point $\mathbf{R}$ lies at the crystal surface. γ_g are the direction cosines of vectors $\mathbf{k}_g$ with respect to the inward surface normal. The coefficient β_g comprehends both the deviation ω and the refraction:[11]

$$\beta_g=\frac{k_g^2-k^2}{K^2}.$$

If the deviation ω is small, the following approximative formula holds:[14]

$$\beta_g\approx 2\omega\exp(2\theta)+\chi_0(1-\gamma_g/\gamma_0). \tag{5}$$

θ is the Bragg angle corresponding to the diffraction vector $\mathbf{g}$, χ_0 is the 0th Fourier coefficient of the crystal polarizability (see below).

As usual, we only consider the two-wave approximation, i.e., in series (2) and (3) we neglect all the terms except those with $\mathbf{g}=0$ or $\mathbf{g}=\mathbf{h}$. We replace the electron density $\rho(\mathbf{r})$ with the crystal polarizability[14]

$$\chi(\mathbf{r})\approx\rho(\mathbf{r})r_{\mathrm{el}}/(\pi K^2).$$

Then we get the following final formula for the diffracted amplitude:

$$D(\mathbf{R})=D_{\mathrm{inc}}\pi CK\chi_h\exp(-2\pi i\kappa_{0x}X)$$
$$\times\int_{l_h(\mathbf{R})} d\mathbf{r}\exp(\pi iK\beta_h z/\gamma_h)\exp[2\pi i\mathbf{h}\cdot\mathbf{u}(\mathbf{r})]. \tag{6}$$

Here $\mathbf{R}=(X,Y,0)$ is the observation point (we have restricted ourselves to the Bragg case of diffraction). The component of vector $\boldsymbol{\kappa}_0$ parallel with the crystal surface is denoted κ_{0x}, it is connected with ω by

$$\kappa_{0x}=-K\gamma_0\omega. \tag{7}$$

Formula (6) has been derived in Ref. 15 by a different procedure.

It is worth mentioning that Eq. (6) can also be obtained as a kinematical limit of an expression for the wave diffracted by a distorted crystal within the dynamical diffraction theory.[11,16] This can be done by calculating the limit $E\to 0$, where E is the static Debye–Waller factor.

III. RANDOMLY DEFORMED CRYSTALS

In most cases the characteristic size of crystal defects is much smaller than the size of the irradiated sample volume V. Then, many defects occur in V and the signal measured during an x-ray experiment can be considered averaged over all macroscopic nonresolvable defect configurations. This averaging we denote by $\langle\ \rangle$. Then, the deformation field $\mathbf{u}(\mathbf{r})$ and the diffracted amplitude $D(\mathbf{R})$ can be treated as random quantities. Moreover, we assume that the measured signal does not change during shifting the sample across the primary beam, i.e., the sample and the diffracted wave are laterally homogeneous.

All the measured quantities can be described using the mutual coherence function (MCF) $\Gamma(\mathbf{R},\mathbf{R}')$ of the diffracted wave:[17]

$$\Gamma(\mathbf{R},\mathbf{R}')=\langle D(\mathbf{R})\,D(\mathbf{R}')^*\rangle. \tag{8}$$

From (6) we get

$$\Gamma(\mathbf{R},\mathbf{R}')=I_{\rm inc}(\pi CK|\chi_h|)^2\exp[-2\pi i\kappa_{0x}(X-X')]\times\int_{l_h(\mathbf{R})}d\mathbf{r}\int_{l_h(\mathbf{R}')}d\mathbf{r}'\exp[\pi iK(\beta_h z-\beta_h^* z')/\gamma_h]\times G(\mathbf{r},\mathbf{r}'), \tag{9}$$

where

$$G(\mathbf{r},\mathbf{r}')=\langle\exp[2\pi i\mathbf{h}\cdot(\mathbf{u}(\mathbf{r})-\mathbf{u}(\mathbf{r}'))]\rangle \tag{10}$$

is the correlation function of the random deformation field $\mathbf{u}(\mathbf{r})$ and $I_{\rm inc}=|D_{\rm inc}|^2$ is the intensity of the primary beam.

The MCF can be splitted into two parts:

$$\Gamma(\mathbf{R},\mathbf{R}')=\langle D(\mathbf{R})\rangle\langle D(\mathbf{R}')\rangle^*+\langle(D(\mathbf{R})-\langle D(\mathbf{R})\rangle)(D(\mathbf{R}')-\langle D(\mathbf{R}')\rangle)^*\rangle. \tag{11}$$

The first term on the right-hand side expresses the coherent part and the second term the partially coherent part of MCF. If the sample is irradiated by a plane monochromatic wave, the coherent part of MCF corresponds to the plane component of the diffracted wave, the partially coherent part describes the diffusely scattered (i.e., divergent) component.

In the case of laterally homogeneous waves there is a direct connection between MCF and the angular intensity distribution in the diffracted wave:

$$\tilde{I}(\mathbf{p})=\int_S d(\mathbf{R}-\mathbf{R}')\Gamma(\mathbf{R}-\mathbf{R}')\exp[2\pi i\mathbf{p}\cdot(\mathbf{R}-\mathbf{R}')]. \tag{12}$$

The integration in this formula is performed over the surface S of the crystal, thus the wave vector $\mathbf{p}$ is parallel to this surface. The physical meaning of $\tilde{I}(\mathbf{p})$ is obvious. The diffracted wave is represented by a superposition of plane components. $\tilde{I}(\mathbf{p})$ is the intensity of a component, whose wave vector is

$$(K_{hx}^B+p_x,p_y,K_{hz}),$$

where $\mathbf{K}_h^B=\mathbf{K}_0^B+\mathbf{h}$ and the z component K_{hz} must be chosen so that the wave vector length $\sqrt{(K_{hx}^B+p_x)^2+p_y^2+K_{hz}^2}$ equals the vacuum wave vector length $K=1/\lambda$.

As an example, let us consider a special type of defects without any correlation of the deformation field. After a straightforward calculation we find that the incoherent component of MCF is zero and for the angular intensity distribution we get

$$\tilde{I}(\mathbf{p})=\text{const}\,\delta(p_x-\kappa_{hx})\delta(p_y).$$

Thus, the diffracted wave is plane and its wave vector is $\mathbf{K}_h^B+\boldsymbol{\kappa}_h$. Its deviation $\boldsymbol{\kappa}_h$ depends on ω, on the x-ray refraction, and on the diffraction asymmetry.

The above theory is applicable for homogeneously strained layers as well. The homogeneous deformation of the layer only causes a shift of the diffusely scattered intensity distribution $\tilde{I}$ in the reciprocal plane without any distortion of its contours. In the case of bent samples the assumption of the crystal homogeneity is not valid and the theory cannot be used. However, the influence of the sample bending strongly depends on the size of the irradiated sample surface. If the irradiated spot is small enough, the change of the angle of incidence of x rays due to the bending is small compared with the width of the layer reflection curve and the sample bending is completely negligible.

IV. SIMULATION OF DIFFRACTION MEASUREMENTS

In the previous section we found explicit formulas for MCF of the wave diffracted on a crystal with randomly distributed small defects. We demonstrated that its Fourier transformation represents the angular distribution of the diffracted intensity. In this section we connect these results with quantities measured in diffractometry experiments.

Two different experimental arrangements are used: Double crystal diffractometry (DC) and triple crystal diffractometry (TC). In DC the sample is irradiated by a nearly parallel and nearly monochromatic x-ray beam and the detector registrates the entire diffracted wave regardless of its direction. In TC the detector only measures the intensity of such diffracted components that can penetrate the narrow angular aperture of the detector. The width of this aperture (in the incidence plane) is limited by the width of the reflection curve of the third crystal (analyzer), perpendicular to that plane it is only limited by the size of the entrance detector window and the distance sample detector (if no Soller slit is used). As usual, we can assume that this height is large and thus the detector is not sensitive to the y component of the deviation $\mathbf{p}$.

A. Double crystal diffractometry

The intensity measured in the DC arrangement can simply be obtained from Eq. (9) putting $\mathbf{R}=\mathbf{R}'$:

$$I(\mathbf{R})=\Gamma(\mathbf{R},\mathbf{R}). \tag{13}$$

If the sample is laterally homogeneous, i.e., if

$$G(\mathbf{r},\mathbf{r}')=G(x-x',y-y';z,z')$$

holds, it can be demonstrated that $\Gamma(\mathbf{R},\mathbf{R}')=\Gamma(\mathbf{R}-\mathbf{R}')$ and, therefore the diffracted intensity does not depend on $\mathbf{R}$. The only problem to solve is to consider the influence of finite angular width and finite spectral width of the primary beam. The spectral width can be assumed small so that all the quantities depending slowly on λ (χ_h, θ, γ_h, etc.) can be considered constant. The spectral width then acts as an additional angular divergence of the primary beam.

In the following we denote $\mathcal{R}_1^{\sigma,\pi}(\phi)$ the reflectivities of the crystal collimator (the first crystal in DC) for σ and π polarizations as a function of the exit angle ϕ of the x-ray beam. This quantity includes the influence of the spectral width of the primary beam as well. $C_{1,2}^{\sigma,\pi}$ is the value of the polarization factor C for the 1st and the 2nd crystal (sam-

ple) and for σ and π polarizations. $\mathscr{R}_2^{\sigma,\pi}(\omega)$ is the reflectivity of the beam diffracted by the sample as a function of ω if the sample is irradiated by a linearly polarized wave in σ and π polarizations, respectively, i.e., $\mathscr{R}_2 = I/I_{\text{inc}}$. Then the signal measured in the DC arrangement is[14]

$$\mathscr{R}_{\text{DC}}(\omega) = \frac{\int_{-\infty}^{\infty} d\phi [\mathscr{R}_1^{\sigma}(\phi)\mathscr{R}_2^{\sigma}(\phi+\omega) + \mathscr{R}_1^{\pi}(\phi)\mathscr{R}_2^{\pi}(\phi+\omega)]}{\int_{-\infty}^{\infty} d\phi [\mathscr{R}_1^{\sigma}(\phi) + \mathscr{R}_1^{\pi}(\phi)]}. \tag{14}$$

In the kinematical approximation $\mathscr{R}_2$ is proportional to the square of the polarization factor, thus, $\mathscr{R}_2^{\pi} = \mathscr{R}_2^{\sigma} \cdot (C_2^{\pi})^2$. If the diffraction on the first crystal is not too asymmetric, its integrated reflectivity $\int \mathscr{R}_1 \, d\phi$ is proportional to the polarization factor.[14] Then Eq. (14) can be simplified

$$\mathscr{R}_{\text{DC}}(\omega) \approx C_{\text{eff}} \frac{\int_{-\infty}^{\infty} d\phi \, \mathscr{R}_1^{\sigma}(\phi)\mathscr{R}_2^{\sigma}(\phi+\omega)}{\int_{-\infty}^{\infty} d\phi \, \mathscr{R}_1^{\sigma}(\phi)}, \tag{15}$$

where the effective polarization factor C_{eff} is

$$C_{\text{eff}} = \frac{1 + C_1^{\pi}(C_2^{\pi})^2}{1 + C_1^{\pi}}. \tag{16}$$

Equations (9), (13), and (15) can be used for simulating a DC measurement in the following steps:

Knowing the explicit form of the correlation function G we get the MCF using Eq. (9).

According to (13) we obtain the diffracted intensity as a function of the angular deviation ω of the sample.

Performing the convolution (14) or (15) we get the DC rocking curve.

B. Triple crystal diffractometry

Since the angular divergence of the diffusely scattered wave is usually broader than the reflection curve of a perfect crystal, we neglect the influence of the divergence and the spectral width of the primary beam and we assume the angular width of the entrance detector aperture in the plane of incidence very small. Then, the sample is irradiated by a plane monochromatic wave and the detector registrates the sum of the intensities $\tilde{I}(\mathbf{p})$ over all possible values p_y. The measured signal $\mathscr{R}_{\text{TC}}$ is then a function of the angular deviation ω of the sample from its Bragg position and of the angular position ω' of the entrance detector aperture (ω' is the angular position of the analyzing crystal). The zeros on the ω, ω' axes are chosen so that $\mathscr{R}_{\text{TC}}$ has a maximum for $\omega = \omega' = 0$. Then

$$\mathscr{R}_{\text{TC}}(\omega,\omega') = \frac{1}{I_{\text{inc}}} \int_{-\infty}^{\infty} dp_y \tilde{I}(p_x,p_y). \tag{17}$$

The angular intensity distribution $\tilde{I}(\mathbf{p})$ depends on ω, ω'. Its dependence on ω is contained in β_h and κ_{0x} according to Eqs. (5) and (7), the angle ω' is included in p_x. Not too far from RELP p_x can be expressed as

$$p_x = K\gamma_h(\omega' - \omega). \tag{18}$$

The signal $\mathscr{R}_{\text{TC}}$ informs about a distribution of the scattering "strength" in the reciprocal plane parallel with the plane of incidence near RELP. Thus, it is useful to convert the function $\mathscr{R}_{\text{TC}}(\omega,\omega')$ into a distribution of $\mathscr{R}_{\text{TC}}$ in that reciprocal plane. We introduce the coordinates q_1, q_2 in that plane, q_1 axis is parallel with the diffraction vector $\mathbf{h}$, q_2 is perpendicular to it. It follows from geometrical considerations[18] that

$$q_1 = K\cos(\theta)\omega'; \quad q_2 = K\sin(\theta)(2\omega - \omega'). \tag{19}$$

These formulas are only valid near RELP. Far from it the dependence of $q_{1,2}$ on ω, ω' is not linear.[19]

The procedure for calculating the distribution of the diffusely scattered intensity $\mathscr{R}_{\text{TC}}(q_1,q_2)$ consists in the following steps:

Knowing the correlation function $G(\mathbf{r},\mathbf{r}')$ we calculate the MCF according to Eq. (9).

We perform the Fourier transformation (12) and obtain the angular distribution $\tilde{I}(\mathbf{p})$.

We integrate this distribution along the y axis [Eq. (17)]. The resulting quantity is a function of ω [according to (5) and (7)] and p_x, which is a function of ω, ω' (18).

Using (19) we transform $\mathscr{R}_{\text{TC}}$ into a function of coordinates $q_{1,2}$ in the reciprocal lattice plane.

V. MOSAIC STRUCTURE MODEL OF EPITAXIAL LAYERS

In this section we derive an explicit formula for G and calculate the DC reflection curves $\mathscr{R}_{\text{DC}}(\omega)$ and the TC distributions $\mathscr{R}_{\text{TC}}(q_1,q_2)$ for a layer with mosaic blocks.

Let us consider an epitaxial layer containing randomly oriented and randomly placed mosaic blocks. We assume that the crystal lattice in the block is only rotated and not strained, so that the deformation tensor has zero diagonal components. Further, the misorientation of two adjacent blocks is not correlated.

We restrict ourselves to a statistically homogeneous layer, thus all the parameters characterizing the mosaic structure (mean block size, mean square misorientation, etc.) are constant over the whole layer. This could not be true in an actual layer, the influence of an inhomogeneity will be discussed in the next section.

Deriving $G(\mathbf{r},\mathbf{r}')$ for mosaic blocks we follow the procedure known from the statistical theory of x-ray diffraction.[20] If points $\mathbf{r}$, $\mathbf{r}'$ lie in the same block, we get

$$G(\mathbf{r},\mathbf{r}') = \langle \exp\{2\pi i \mathbf{h} \cdot [\boldsymbol{\xi} \times (\mathbf{r} - \mathbf{r}')]\} \rangle,$$

where $\boldsymbol{\xi}$ is the random rotation vector of the block. Let us assume that the lengths of these vectors are distributed normally with zero mean and dispersion Δ^2, their directions are distributed isotropically. Then we obtain

$$G(\mathbf{r},\mathbf{r}') = \exp[-\tfrac{2}{3}(\pi h \Delta\rho)^2], \tag{20}$$

where $\boldsymbol{\rho}$ is the component of vector $\mathbf{r} - \mathbf{r}'$ perpendicular to $\mathbf{h}$.

If points $\mathbf{r}$, $\mathbf{r}'$ lie in different blocks, the shifts $\mathbf{u}(\mathbf{r})$ and $\mathbf{u}(\mathbf{r}')$ are not correlated and

$$G(\mathbf{r},\mathbf{r}') = E^2, \tag{21}$$

where

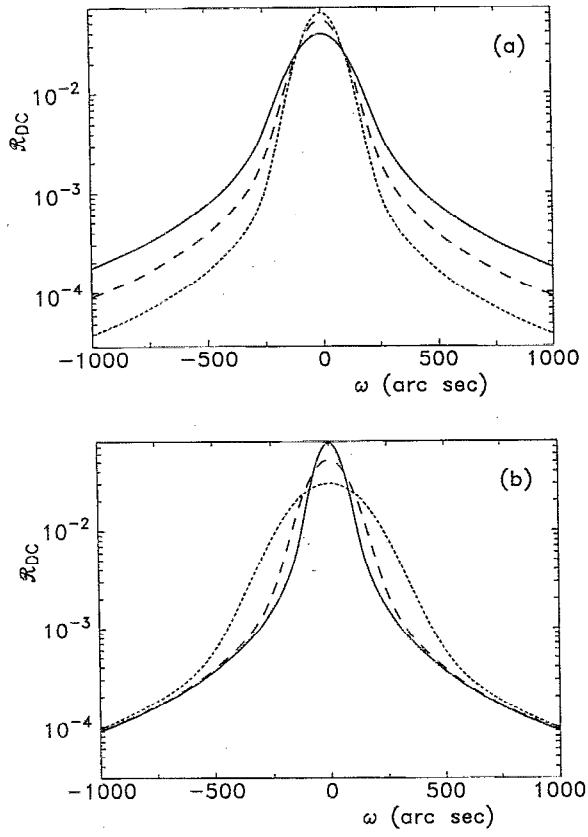

FIG. 1. DC reflection curves of a ZnTe layer (Cu 004 symmetrical Bragg case, layer thickness $T=3$ μm) calculated for various R (part a) and Δ (part b). In part a: $\Delta=100$ arcsec, $R=0.1$ μm (full), 0.2 μm (dashed), and 0.5 μm (dotted). In part b: $R=0.2$ μm, $\Delta=50$ arcsec (full), 100 arcsec (dashed), and 200 arcsec (dotted).

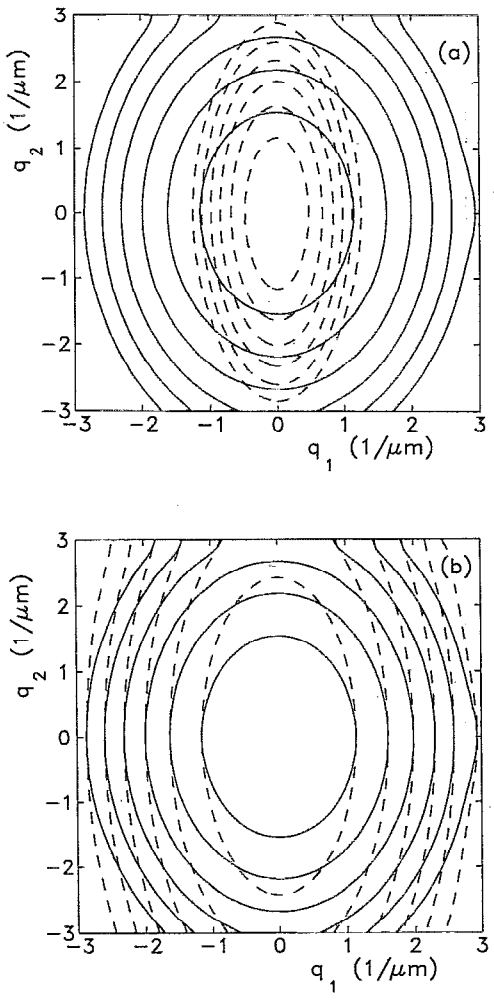

FIG. 2. TC contour maps of diffuse x-ray scattering from a 3-μm-thick ZnTe layer (Cu $K\alpha_1$, RELP 002) calculated for various R (part a) and Δ (part b). In part a: $\Delta=100$ arcsec, $R=0.2$ μm (full) and 0.5 μm (dashed). In part b: $R=0.2$ μm, $\Delta=100$ arcsec (full) and 200 arcsec (dashed). Neighboring contours represent the intensity ratio $10^{0.2}$.

$$E=\langle \exp[2\pi i\mathbf{h}\cdot\mathbf{u}(\mathbf{r})]\rangle$$

is the static Debye-Waller factor (assumed constant over the whole volume).

Denoting $P(\mathbf{r},\mathbf{r}')$ the probability of finding both points $\mathbf{r}$, $\mathbf{r}'$ in the same block we get for the correlation function the following relation:

$$G(\mathbf{r},\mathbf{r}')=E^2[1-P(\mathbf{r},\mathbf{r}')]+\exp[-\tfrac{2}{3}(\pi h\Delta\rho)^2]P(\mathbf{r},\mathbf{r}'). \tag{22}$$

The explicit form of P depends on the block shape. In the simplest case we consider spherical blocks with mean radius R. It is shown in the Appendix that

$$P(|\mathbf{r}-\mathbf{r}'|) = \begin{cases} 1-\dfrac{3|\mathbf{r}-\mathbf{r}'|}{(4R)}+\dfrac{(|\mathbf{r}-\mathbf{r}'|/R)^3}{16} & \text{for } |\mathbf{r}-\mathbf{r}'|<2R, \\ 0 \quad \text{for } |\mathbf{r}-\mathbf{r}'|\geqslant 2R. \end{cases} \tag{23}$$

It can be seen that $P=1$ if $\mathbf{r}=\mathbf{r}'$.

From the numerical estimate it follows that $E<10^{-3}$, thus, for reasonable values of R and Δ the coherent component of the diffracted intensity is negligibly small.

Thus, within the model of randomly oriented spherical blocks two parameters characterize the mosaic structure: the mean block radius R and the rms (root-mean-square) misorientation Δ. In the following we show the influence of these parameters on $\mathscr{R}_{DC}$ and $\mathscr{R}_{TC}$. We perform the numerical calculations for the symmetrical 004 Bragg case diffraction on a ZnTe layer, Cu $K\alpha_1$ radiation. Calculating $\mathscr{R}_{DC}$ we neglect the divergence of the primary beam.

Figures 1(a) and 1(b) show the calculated DC reflection curves for various R [Fig. 1(a)] and Δ [1(b)]. It can be seen that R influences mainly the tails of the curves; if R grows the tails decrease. The diffracted intensity can be expressed as an integral of the scattering strength near RELP over the Ewald sphere. If R grows the distribution of the scattering strength gets closer to RELP, hence the intensity diffracted under greater deviations ω diminishes.

From Fig. 1(b) it follows that with increasing Δ the width of the reflection curve (FWHM) grows while its tails remain nearly unchanged.

Figures 2(a) and 2(b) present the distributions $\mathscr{R}_{TC}(q_1,q_2)$ in the reciprocal lattice plane near RELP. It is obvious that the size of the scattering strength "cloud" in

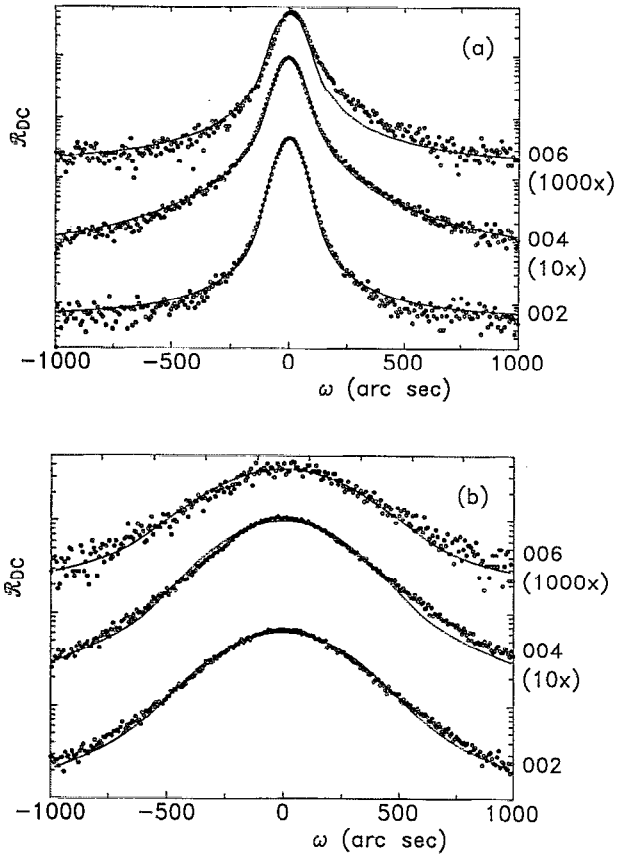

FIG. 3. Experimental (circles) and calculated (lines) DC reflection curves of a ZnTe layer before thinning ($T=6.2$ μm, part a) and after the last thinning step ($T=1.4$ μm, part b).

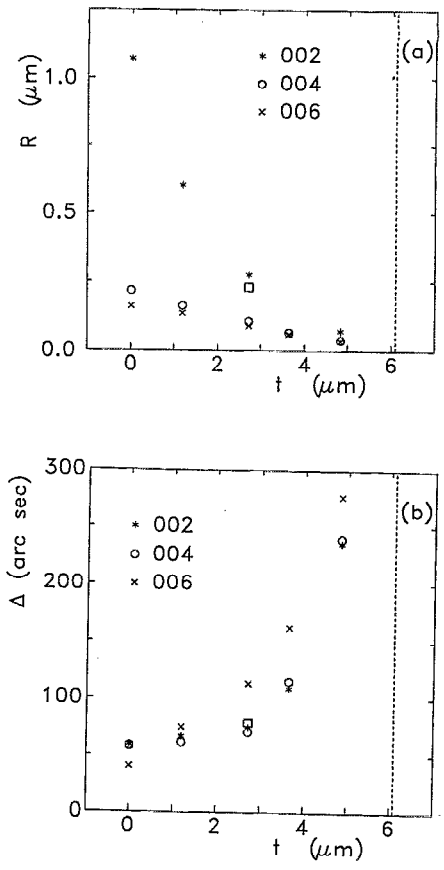

FIG. 4. Dependences of R (part a) and Δ (part b) on the removed layer thickness t obtained from the fits of the experimental DC curves with the theory. The dotted line illustrates the layer-substrate interface ($T=6.2$ μm); squares represent the values from the fit of the TC contour map (see Fig. 5). The relative errors of R and Δ are $\sim 10\%$.

the q_1 direction (i.e., parallel with the diffraction vector $\mathbf{h}$) depends on R, while that in the q_2 direction depends both on R and on Δ.

VI. EXPERIMENTS

In this section we demonstrate the applicability of the above theory for investigating the real structure of epitaxial layers. We measured the DC reflection curves of a ZnTe heteroepitaxial layer after several steps of its chemical thinning. The layer has been grown by hot wall epitaxy on a GaAs substrate. For the measurements we used a Bartels four-crystal Ge monochromator in the 220 setting as the first crystal. In addition, after two steps of thinning we measured the TC diffuse scattering distribution $\mathcal{R}_{TC}(q_1,q_2)$ near RELP of the layer. For the DC measurements we used symmetrical 002, 004, and 006 Bragg case diffractions (Cu $K\alpha_1$ radiation), the TC measurement was performed in the symmetrical 004 diffraction.

It has been proved by DC measurements that the layer was nearly fully relaxed, i.e., the tetragonal distortion of the layer elementary cells was negligible.

Figures 3(a) and 3(b) show the measured (circles) and fitted (lines) DC reflection curves before the first thinning (the layer thickness $T=6.2$ μm) and after the last thinning ($T=1.4$ μm). From the fits we obtained the dependences of the parameters R and Δ on the thickness t of the removed layer. This dependence is plotted in Figs. 4(a) and 4(b).

Figure 5 shows the $\mathcal{R}_{TC}$ contour maps measured after

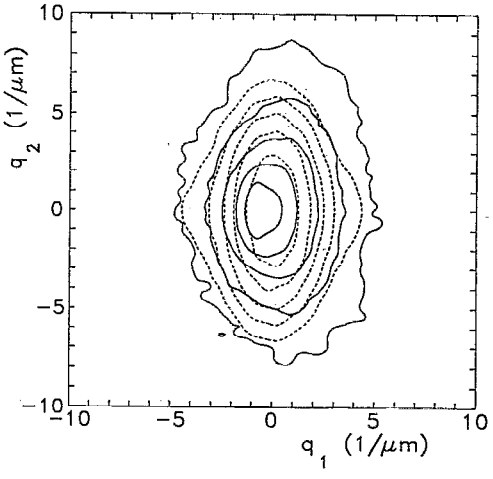

FIG. 5. TC contour map measured near RELP 004 after the second thinning step (full) and its simulation (dashed). The neighboring contours represent the intensity ratio $\sqrt{10}$.

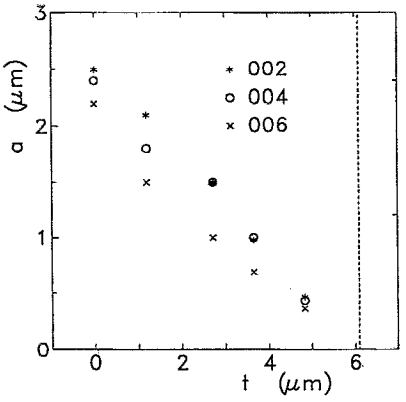

FIG. 6. Mean distance a of adjacent dislocations estimated from FWHMs of measured DC curves as a function of removed layer thickness t. The relative error of a is $\sim 15\%$.

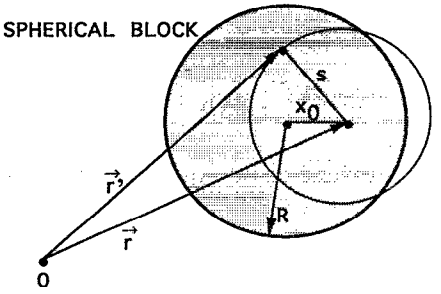

FIG. 7. Sketch for deriving $P(s)$.

the second thinning step ($T=3.5$ μm) and calculated using the defect parameters following from the numerical fit with the theory. The values of R and Δ following from the fit are plotted in Figs. 4(a) and 4(b) again.

VII. DISCUSSION

The experimental DC curves compare well with the theory. The distribution of the diffuse scattering strength measured by TC exhibits a slight asymmetry, probably due to a residual strain gradient near the substrate. The residual strain gradient was not considered in our model and it affected unfavorably the accuracy of determining R and Δ by the fitting procedure. Nevertheless, the layer was nearly fully relaxed and therefore the residual stress was not big enough to bend the whole sample. This statement is supported by the form of the TC contour maps; the substrate peak in the measured map was circularly symmetrical and its width was comparable with the divergence of the primary beam ~ 12 arcsec.

The fact that R and Δ depend on t disagrees with the assumption about the layer homogeneity performed in Sec. V. R and Δ found from the fits represent some effective values averaged over the penetration depth of the primary x-ray beam. This depth can be estimated as $1/\mu_{\text{eff}}$, where μ_{eff} is the effective linear absorption coefficient. For the Cu 002 diffraction the penetration depth is about 2 μm, while for Cu 006 it is nearly 7 μm. This could be the reason for the differences between the R and Δ values found from different diffractions. The values found for 002 diffraction represent the best estimates for the true dependences $R(t)$, $\Delta(t)$.

The above theory can be applied if the layer is thin enough and if the diffraction in the substrate can completely be neglected. The latter condition means that the scattering strength "clouds" near RELPs of the layer and the substrate shoud not overlap. This is fulfilled only for greater lattice misfits of the layer and substrate.

It is well known that heteroeptiaxial layers contain defects of various types (misfit dislocations, threading dislocations, various precipitates, etc.). We described the defect structure using the mosaic defect model; thus, the connection of the mosaic blocks with the actual defect structure is only indirect. The values of R and Δ found by the fit represent rather some effective values than true defect parameters. The above description of the diffraction process using MCF is general and it can be used also for other defect types, provided that the correlation function $G(\mathbf{r},\mathbf{r}')$ of the deformation field is known.

The connection of our defect model with the conception of randomly distributed dislocations can easily be demonstrated. From FWHMs of DC curves the dislocation density D can be estimated.[4] Figure 6 represents the mean distance a of adjacent dislocations (calculated by $a=1/\sqrt{D}$) as a function of t. Comparing with Fig. 4(a) we find that a agrees approximately with mean block diameter $2R$. Therefore, the mosaic block used in our model corresponds with the undeformed part of the crystal lattice between neighboring dislocations.

From Figs. 4(a) and 4(b) and 6 it is obvious that the structural quality of the layer gets better towards the free surface. This agrees with our previous results.[1,2]

In our model we considered neither the surface relaxation of the stresses introduced by the defects nor the anisotropy of the defect shapes. Further improvement of the defect model could include possible strain in mosaic blocks and various block shapes.

VIII. CONCLUSION

We developed the theoretical description of the x-ray diffraction in thin layers containing small randomly distributed defects. Our approach is based on the kinematical approximation of the diffraction theory and on the optical coherence formalism. The theory enables us to calculate both the DC reflection curves and the TC contour maps of diffuse x-ray scattering.

The theory has been used for investigating the mosaic structure of epitaxial layers. We showed that the statistical parameters of the defects (block size and block misorientation) can be determined from DC reflection curves. We demonstrated that the theory explains the form of experimental TC contour maps and a qualitative agreement with the experimental maps was achieved. The conception of mosaic blocks is only a rough model of actual defect struc-

ture in a heteroepitaxial layer. For a more detailed study of the defects an application of several independent methods is inevitable.

APPENDIX

In the following we derive Eq. (23) for the probability P of finding two points $\mathbf{r}$ and $\mathbf{r}'$ in the same mosaic block. Let us assume blocks of spherical form with radius R. Then P only depends on $s=|\mathbf{r}-\mathbf{r}'|$.

Let us put one point (say $\mathbf{r}$) into the distance x_0 from the block center ($x_0<R$) and the other ($\mathbf{r}'$) into the distance s from the first one. The probability $P_c(x_0,s)$ of finding point $\mathbf{r}'$ in the same block is then proportional to the area of that part of the spherical surface with centre in $\mathbf{r}$ and radius s, which lies inside the block (see Fig. 7).

After a simple but lengthy calculation we obtain

$$P_c(x_0,s)=\begin{cases}1 & \text{for } x_0<R-s \text{ and } s<R\\ (R^2-s^2+2sx_0-x_0^2)/(4x_0s) & \text{for } |R-s|<x_0<R \text{ and } s<2R\\ 0 & \text{for } x_0<s-R \text{ and } R<s<2R\\ 0 & \text{for } s>2R.\end{cases} \tag{A1}$$

$P_c(x_0,s)$ is a conditional probability, therefore for probability $P(s)$ we get

$$P(s)=\frac{\int_0^R dx_0 P_c(x_0,s)P'(x_0)}{\int_0^R dx_0 P'(x_0)}, \tag{A2}$$

where $P'(x_0)$ is the probability of putting the point $\mathbf{r}$ into the distance x_0 from the block center. It is proportional to the spherical surface area $4\pi x_0^2$.

Putting from (A1) into (A2) we obtain the final formula (23) for the probability $P(s)$.

[1] E. Abramof, K. Hingerl, A. Pesek, and H. Sitter, Semicond. Sci. Technol. **6**, A80 (1991).
[2] G. Kudlek, N. Presser, J. Gutowski, K. Hingerl, E. Abramof, A. Pesek, H. Pauli, and H. Sitter, J. Cryst. Growth **117**, 290 (1992).
[3] P. Demeester, A. Ackaert, G. Coudenys, I. Moerman, L. Buydens, I. Pollentier, and P. Van Daele, Prog. Cryst. Growth Charact. **22**, 53 (1991).
[4] P. Gay, P. B. Hirsch, and A. Kelly, Acta Metall. **1**, 315 (1953).
[5] A. A. Lomov, P. Zaumseil, and U. Winter, Acta Cryst. A **41**, 223 (1985).
[6] P. F. Fewster, J. Appl. Cryst. **22**, 64 (1989).
[7] P. F. Fewster, in *Heteroepitaxial Approaches in Semiconductors; Lattice Mismatch and its Consequences*, Vol. 89-5, edited by T. Macrander and T. J. Drummond (Electrochemical Society, Pennington, NJ, 1989), pp. 278–286.
[8] P. F. Fewster, Appl. Surf. Sci. **50**, 9 (1991).
[9] J. H. van der Merwe, Crit. Rev. Solid State Mater. Sci. **17**, 187 (1991) and citations therein.
[10] R. G. Newton, *Scattering Theory of Waves and Particles* (McGraw–Hill, New York, 1966).
[11] S. Takagi, J. Phys. Soc. Jpn. **26**, 1239 (1969).
[12] M. Born and E. Wolf, *Principles of Optics* (Pergamon, London, 1959).
[13] See, for instance, L. V. Azároff, R. Kaplow, N. Kato, R. J. Weiss, A. J. C. Wilson, and R. A. Young, *X-Ray Diffraction* (McGraw–Hill, New York, 1974).
[14] Z. G. Pinsker, *Dynamical Scattering of X-Rays in Crystals* (Springer, Berlin, 1978).
[15] P. V. Petrashen, Fiz. Tverdogo Tela **17**, 2814 (1975).
[16] A. M. Afanasev and V. G. Kohn, Acta Cryst. A **27**, 421 (1971).
[17] V. Holý and K. T. Gabrielyan, Phys. Status Solidi B **140**, 39 (1987).
[18] A. Iida and K. Kohra, Phys. Status Solidi A **51**, 533 (1979).
[19] E. Koppensteiner (to be published).
[20] N. Kato, Z. Naturforsch **37a**, 485 (1982) and citations therein.